

# Optimizing Individual-based Modelling: A Grid-based Approach to Computationally Efficient Microbial Simulations

Ihab Hashem<sup>a</sup>, Jian Wang<sup>a</sup> and Jan F.M. Van Impe<sup>a\*</sup>

<sup>a</sup> BioTeC+ KU Leuven, Department of Chemical Engineering, Gent, Belgium

\* Corresponding Author: [jan.vanimpe@kuleuven.be](mailto:jan.vanimpe@kuleuven.be).

## ABSTRACT

Individual-based modeling (IbM) has emerged as a powerful approach for studying microbial populations, offering a bottom-up framework to simulate cellular behaviors and their interactions. Unlike continuum-based models, IbM explicitly captures the heterogeneity and emergent dynamics of microbial communities, making it invaluable for studying spatially structured phenomena such as nutrient competition, biofilm formation, and colony interactions. However, IbM faces significant computational challenges, particularly in resolving spatial overlaps during simulations of large microbial populations. Traditional approaches, such as pairwise comparisons or kd-trees, are computationally expensive and scale poorly with population size. The Discretized Overlap Resolution Algorithm (DORA) introduces a novel grid-based solution to overcome these limitations. By encoding spatial information into an occupancy matrix, DORA achieves a time complexity of  $O(N)$ , enabling efficient resolution of overlaps while maintaining spatial fidelity. To validate its capabilities, we applied DORA to a case study of microbial colony merging. Two scenarios were tested: (1) colonies inoculated 40  $\mu\text{m}$  apart merged at the center due to nutrient depletion, and (2) colonies inoculated 120  $\mu\text{m}$  apart remained separate, with a no-growth zone forming between them. In both cases, DORA replicated observed phenomena with high accuracy and demonstrated linear scalability, significantly reducing simulation time compared to traditional methods. DORA's computational efficiency and scalability position it as a robust tool for large-scale IbM simulations, advancing our ability to study complex microbial systems in diverse ecological and industrial contexts.

**Keywords:** Individual-based modeling, Grid-based algorithm, microbial ecology

## INTRODUCTION

Microbial populations are integral to a wide range of biochemical engineering applications, including wastewater treatment, bioreactor optimization, and the formation of biofilms on industrial and medical surfaces. Understanding and predicting the behavior of these populations require robust modeling frameworks capable of capturing individual cellular behaviors and the emergent dynamics of entire populations. Among these frameworks, Individual-based modeling (IbM) has emerged as a powerful computational framework for studying microbial systems. Unlike continuum-based models, which rely on averaged properties, IbM explicitly captures the behavior and interactions of individual cells, enabling a

bottom-up analysis of population-level dynamics. By modeling each cell's local interactions, growth, division, and motility, IbM provides insights into how spatial structure influences social behaviors such as nutrient competition, metabolic cooperation, and quorum sensing [1,2]. These capabilities make IbM particularly valuable in industries where microbial interactions critically impact process performance, stability, and safety, such as food preservation, bioreactor optimization, wastewater treatment, and synthetic biology. By bridging microscale cell behavior with macroscale community dynamics, IbM offers practical insights into microbial processes across diverse natural, medical, and industrial applications [3].

Despite its strengths, IbM faces significant computational challenges, particularly when applied to large

microbial populations. A primary bottleneck lies in resolving spatial overlaps between cells, a critical step in maintaining spatial fidelity during simulations. Traditional methods for resolving overlaps often rely on pairwise comparisons between cells, relying on data structures such as kd-trees. These kd-trees recursively partition the simulation space to reduce the complexity of neighbor searches to  $O(\log N)$ , a substantial improvement over earlier array-based methods with  $O(N^2)$  complexity. However, while such complexity is efficient in theory, it still poses a significant computational burden when considering the exponential growth of microbial populations in simulations. This rapid growth exacerbates the demands of spatial overlap resolution, particularly in dynamic simulations where cells grow, divide, and move frequently [4][5].

To address these challenges, we developed the Discretized Overlap Resolution Algorithm (DORA), a novel grid-based method designed to optimize the overlap resolution process. By encoding the spatial information of cells into a grid-based occupancy matrix, which then guides cellular movements, DORA circumvents the need for pairwise comparisons entirely, reducing computational complexity to  $O(N^2)$ . The algorithm operates in three main steps: (i) forward translation, where the spatial information of cells is encoded into an occupancy matrix; (ii) overlap resolution, which employs a diffusion-like process to iteratively redistribute excess occupancy values; and (iii) backward translation, where the resolved grid data are converted back into movement vectors for individual cells. This grid-based framework hence improves computational efficiency and allows the implementation of large-scale simulations [6].

DORA was integrated into MICRODIMs, an in-house lbM platform [7][8] built on the Repast Symphony toolkit [9]. MICRODIMs provides a flexible framework for simulating microbial growth dynamics, nutrient diffusion, and biofilm formation [10]. The integration of DORA significantly enhanced MICRODIMs's performance and enabled it to handle large-scale simulations of microbial colonies and biofilms within computationally feasible timeframes.

To further test DORA's performance and its applicability under biologically relevant conditions, we introduced a stochastic displacement component prior to the overlap resolution step. This component captures inherent biological variability, such as microbial motility and environmental fluctuations, thereby enhancing the realism of the simulations. As a case study, we applied DORA to simulate the merging of two microbial colonies—a process influenced by complex factors such as the distance between colonies, nutrient availability, and medium diffusivity [8]. This scenario presents a challenging test case for spatial fidelity, requiring the algorithm to accurately capture the conditions under which colony merging occurs. Our results demonstrated that DORA effectively

modeled the process, providing high-fidelity representations of colony merging dynamics across different environmental conditions.

## MATERIALS AND METHODS

### The Discretized Overlap Resolution Algorithm (DORA)

Resolving spatial overlaps in lbMs traditionally relies on data structures such as arrays or kd-trees. Arrays store cell positions directly but require computationally expensive pairwise comparisons (complexity  $O(N^2)$ ) [4]. Kd-trees improve efficiency by recursively partitioning space, reducing neighbor searches to  $O(\log N)$  per query. However, dynamic simulations require frequent tree rebalancing due to cell movement and growth, increasing computational and memory overhead, especially at high cell densities [5].

DORA overcomes these limitations by discretizing the simulation space into an occupancy matrix, avoiding pairwise comparisons entirely and achieving an overall complexity of  $O(N)$ . Additionally, DORA can incorporate a stochastic motion step before overlap resolution to introduce biologically relevant variability, such as microbial motility.

### Stochastic Motion

Before executing the main steps of the DORA algorithm, a stochastic displacement is applied to each cell. A random displacement vector  $(\Delta x, \Delta y)$  is sampled from a Gaussian distribution:

$$\Delta x, \Delta y \sim N(0, \sigma^2) \quad (1)$$

where  $\sigma$  represents the standard deviation of the displacement. The new cell positions are calculated as:

$$x' = x + \Delta x \quad (2)$$

$$y' = y + \Delta y \quad (3)$$

subject to the constraints of the simulation environment. This stochastic motion introduces biologically relevant noise into the simulation, simulating random fluctuations in cell movements.

### Forward Translation

The next step maps the spatial attributes of cells onto a discretized occupancy matrix,  $\Omega$ , which divides the simulation environment into grid units of width  $w$  and height  $h$ . Each unit in the grid stores a value representing the fraction of its area occupied by cells.

For a cell centered at  $(x_c, y_c)$  with radius  $r$ , its boundaries relative to the grid are calculated as:

$$x_{left/right} = x_c \pm \frac{r}{w} \quad (5)$$

$$y_{bottom/top} = y_c \pm \frac{r}{h} \quad (6)$$

The occupancy of a grid unit  $(i, j)$  by cell  $k$  is determined by the overlap between the cell and the grid unit, calculated as:

$$\Omega_{\{i,j\}}^k = \frac{\text{horizontal overlap} \times \text{vertical overlap}}{w \times h} \quad (7)$$

The horizontal overlap is computed as:

$$\max(0, \min(i + 1, x_{\text{right}}) - \max(i, x_{\text{left}})) \quad (8)$$

and similarly for the vertical overlap:

$$\max(0, \min(j + 1, j_{\text{top}}) - \max(j, x_{\text{bottom}})) \quad (9)$$

The total occupancy of grid unit  $(i, j)$  is the sum of contributions from all cells overlapping the unit:

$$\Omega[i][j] = \sum_k \Omega_{ij}^k \quad (10)$$

Values of  $\Omega[i][j] < 1$  indicate under-occupied units,  $\Omega[i][j] = 1$  represents fully occupied units, and  $\Omega[i][j] > 1$  identifies over-occupied units requiring resolution.

## Overlap Resolution

Overlap is identified wherever  $\Omega[i][j] > 1$ . An excess matrix  $E$  is defined to quantify the surplus occupancy:

$$E_{ij} = \max(0, \Omega_{ij} - 1) \quad (11)$$

The algorithm redistributes excess values iteratively across neighboring grid units within the Von Neumann neighborhood  $N_{ij}$ , which includes the four adjacent units (up, down, left, and right). The redistribution is governed by:

$$\Omega'_{ij} = \Omega_{ij} - \alpha \times \left( E_{ij} - \frac{1}{4} \sum_{(k,l) \in N_{ij}} E_{kl} \right) \quad (12)$$

where  $\alpha$  is a diffusivity factor that ensures numerical stability. A motion tensor  $M$  is used to track the directional displacements required to resolve overlaps. For a grid unit  $(i, j)$  and a neighboring unit  $(k, l)$ , the displacement in direction  $d$  is updated as:

$$M_{ij}^d(t+1) = M_{ij}^d(t) + \alpha \times \frac{1}{4} (E_{ij} - E_{kl}) \quad (13)$$

## Backward Translation

In the final step, the computed displacements in the motion tensor  $M$  are translated back to movement vectors for individual cells. For a grid unit  $(i, j)$  occupied by a cell, the local movement vector is:

$$(v_{x_{ij}}, v_{y_{ij}}) = (M_{ij}^{\text{right}} - M_{ij}^{\text{left}}, M_{ij}^{\text{top}} - M_{ij}^{\text{bottom}}) \quad (14)$$

For cells spanning multiple grid units, the overall movement vector is determined by summing contributions from all occupied units:

$$V_x = \sum_{(i,j) \in \text{Cell's grid units}} v_{x_{ij}} \quad (15)$$

$$V_y = \sum_{(i,j) \in \text{Cell's grid units}} v_{y_{ij}} \quad (16)$$

To optimize computational efficiency, the simulation dynamically determines the active simulation area, restricting calculations to the region where cells are present. Let  $x_c$  and  $y_c$  denote the coordinates of all cells. To optimize computational efficiency, the simulation restricts calculations to the active region, defined as:

$$\text{Left, Right} = \max(0, \min(x_c) - \Delta),$$

$$\min(W, \max(x_c) + \Delta) \quad (17)$$

where  $\Delta$  represents a buffer margin added around the bounding box to prevent edge effects, and  $W$  is the total width of the simulation domain. And similarly, for  $\text{Bottom, Top}$ . The algorithm operates only within the box:

$$B = \{ (x, y) \mid \text{Left} \leq x \leq \text{Right}, \text{Bottom} \leq y \leq \text{Top} \} \quad (18)$$

By dynamically restricting calculations to  $B$ , DORA minimizes unnecessary computations, improving efficiency.

DORA is implemented in the MICRODIMS platform, built on the Repast Symphony toolkit. The simulation environment is discretized into a  $600 \times 600 \mu\text{m}$  grid with periodic boundary conditions. Cell growth follows Monod kinetics, and substrate diffusion is resolved using the Forward-Time Central-Space (FTCS) scheme. Temporal resolution is achieved by updating cell positions and metabolic processes every 0.01 min.

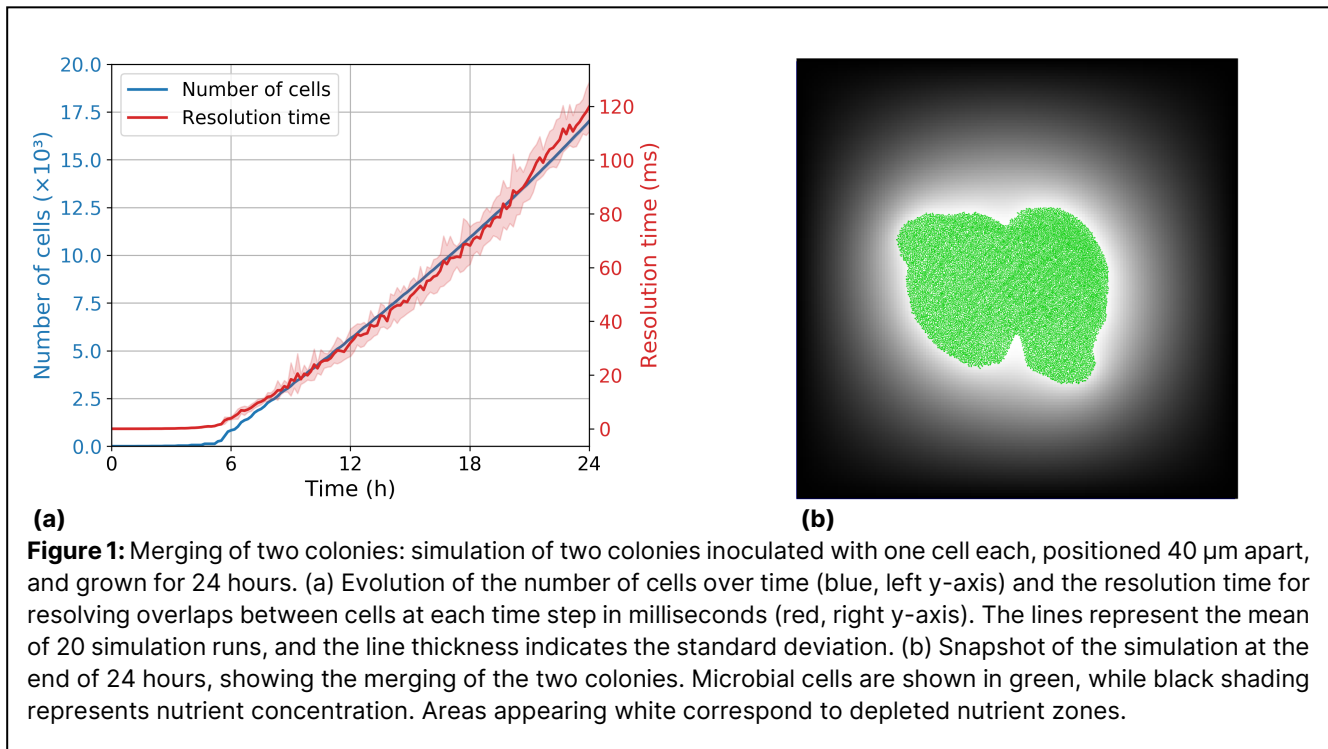
## RESULTS

Modeling cell collisions and resolving spatial overlaps are critical steps in IBM of cells. To test the DORA algorithm's ability to reproduce complex spatial phenomena, we conducted a case study of colony merging, previously explored by Tack et al. [8]. Depending on local conditions, diffusivity, nutrient concentration, inoculation density, and the distance between inocula, colonies close to each other may either merge or remain separate.

### Scenario 1: Merging of Colonies

In the first scenario, we inoculated the medium with two cells positioned  $40 \mu\text{m}$  apart. The results, shown in Figure 1, indicate that the colonies continued to grow until they merged at the center. The DORA algorithm handled spatial resolution effectively during both the growth phase and the merging process, successfully replicating this spatial phenomenon.

In Figure 1(a), we plotted the evolution of the population size and the resolution time required to resolve spatial overlaps at each simulation step over 24 hours. The results represent the mean of 20 simulation runs, with the line thickness indicating the standard deviation. Notably, the growth curve is more linear rather than exponential, which is attributed to the limited diffusivity of the medium. Additionally, the resolution time curve closely follows the population growth, a result of the



algorithm's time complexity of  $O(N)$ . This highlights the efficiency of the DORA algorithm compared to the original array-based overlap resolution method with a time complexity of  $O(N^2)$ . The reduced computational demands decreased the total simulation time to approximately 10 minutes per run, compared to several hours required in the original simulation.

Another observation is the asymmetry between the two colonies despite the symmetric initial conditions. This can be attributed to the stochastic component incorporated into the DORA algorithm, which introduces variability in spatial dynamics and accounts for the variance observed across the simulation runs.

### Scenario 2: Non-Merging of Colonies

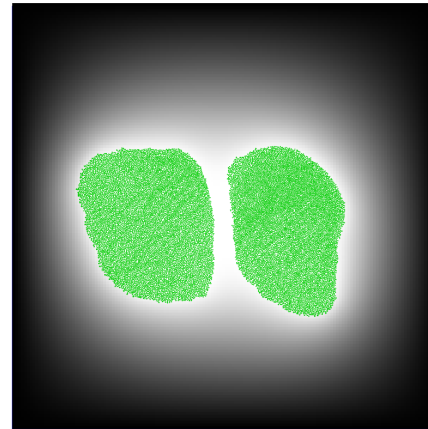
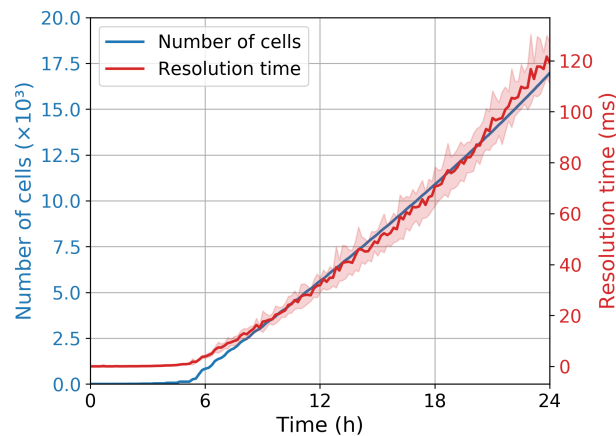
In the second scenario, the two cells were inoculated at 120  $\mu\text{m}$  apart. As shown in Figure 2, the colonies grew by consuming the nutrients in the intercolony region. Due to the larger initial distance, the colonies grew to relatively larger sizes, completely depleting the nutrients between them and creating a no-growth zone in-between that acts as a barrier to merging.

While this scenario is spatially less complex than the merging case, the DORA algorithm successfully replicated the phenomenon. Figure 2(a) presents the mean population size and resolution time for 20 runs, with the standard deviation shown by the line thickness. The growth dynamics and asymmetry between the colonies observed in this scenario were consistent with the first case. The incorporation of stochasticity accounts for the spatial variability and the variance in the results.

The spatial interactions captured by DORA and reproduced in these simulations reflect fundamental microbial behaviors typically observed in structured environments. In such settings, colony growth is shaped by nutrient availability, diffusion constraints, and spatial competition, where interactions occur not only between individual cells but also at the colony level. The observed merging and non-merging results align with previous experimental and modeling studies, which have shown that microbial colonies can either coalesce or remain spatially segregated depending on local resource depletion and diffusivity. For example, studies on *Escherichia coli* K-12 growing in structured media have demonstrated that higher inoculum densities lead to intensified intercolony competition, often resulting in smaller final colony sizes and the formation of distinct separation zones between neighboring populations.

Beyond computational efficiency, the ability to model colony merging and segregation has implications for understanding microbial coexistence and strain diversity. In natural and engineered microbial ecosystems, spatial structuring plays a crucial role in determining whether different strains or species compete, coexist, or evolve specialized niches. By capturing these interactions, DORA provides a valuable framework for exploring how spatial constraints influence microbial diversity, community stability, and ecological succession.

These results demonstrate that the DORA-based lbM efficiently reproduces both merging and non-merging colony behaviors, maintaining high spatial fidelity while significantly reducing computational overhead. This



(a)

(b)

**Figure 2:** Non-merging of two colonies: simulation of two colonies inoculated with one cell each, positioned 120  $\mu\text{m}$  apart, and grown for 24 hours. (a) Evolution of the number of cells over time (blue, left y-axis) and the resolution time for resolving overlaps between cells at each time step in milliseconds (red, right y-axis). The lines represent the mean of 20 simulation runs, and the line thickness indicates the standard deviation. (b) Snapshot of the simulation at the end of 24 hours, showing the two colonies remaining separate and failing to merge. Microbial cells are shown in green, while black shading represents nutrient concentration. A starvation zone emerges between the two colonies, appearing as a white region where nutrients have been fully depleted, preventing further growth and colony merging.

establishes the DORA algorithm as a scalable and reliable tool for modeling complex spatial phenomena in microbial systems.

## CONCLUSION

This study demonstrates the effectiveness of the DORA algorithm in resolving spatial overlaps and replicating complex growth phenomena in microbial simulations. Through the case study of microbial colony merging, DORA was shown to accurately model both merging and non-merging scenarios under varying inoculation distances. By leveraging a grid-based framework with a time complexity of  $O(N)$ , DORA achieved significant reductions in computational overhead compared to traditional methods, enabling faster simulations without sacrificing spatial fidelity. The incorporation of stochastic components introduced biologically relevant variability, further validating the robustness of the algorithm.

By improving the computational feasibility of large-scale simulations, DORA enhances the applicability of lbMs in biochemical engineering, ecological modeling, and bioprocess optimization.

## ACKNOWLEDGEMENTS

This work was supported by the Research Foundation Flanders (FWO) (project G0B4121N to JVI), by the European Commission within the framework of the Erasmus+ Programme (FOOD4S Erasmus Mundus Joint

Master Degree in Food Systems Engineering, Technology and Business 619864-EPP-1-2020-1-BE-EPPKA1-JMD-MOB to JVI), by the European Union's Horizon 2020 research and innovation programme (under the Marie Skłodowska-Curie grant agreement No. 956126 E-MUSE to JW and JVI) and by the European Union's Horizon Europe research and innovation programme (under Grant Agreement No. 101058422 SUPREME - Sustainable nanoParticles Enabled antiMicrobial surfaceE coatings - to IH and JVI).

## REFERENCES

1. Grimm, V. Ten years of individual-based modelling in ecology: what have we learned and what could we learn in the future? *Ecological Modelling*, 115(2-3), 129–148 (1999). [https://doi.org/10.1016/S0304-3800\(98\)00188-4](https://doi.org/10.1016/S0304-3800(98)00188-4)
2. Esser, D. S., Leveau, J. H., & Meyer, K. M. Modeling microbial growth and dynamics. *Applied Microbiology and Biotechnology*, 99, 8831–8846 (2015). <https://doi.org/10.1007/s00253-015-6877-6>
3. Hellweger, F.L., Clegg, R.J., Clark, J.R., Plugge, C.M., & Kreft, J.-U. Advancing microbial sciences by individual-based modelling. *Nature Reviews Microbiology*, 14(7), 461–471 (2016). <https://doi.org/10.1038/nrmicro.2016.62>
4. Kreft, J. U., Picioreanu, C., Wimpenny, J. W., & van Loosdrecht, M. C. Individual-based modelling of biofilms. *Microbiology*, 147(11), 2897–2912 (2001).

- <https://doi.org/10.1099/00221287-147-11-2897>
5. Hellweger, F. L., & Bucci, V. A bunch of tiny individuals—Individual-based modeling for microbes. *Ecological Modelling*, 220(1), 8–22 (2009).  
<https://doi.org/10.1016/j.ecolmodel.2008.09.004>
  6. Hashem, I., Wang, J., & Van Impe, J. A Discretized Overlap Resolution Algorithm (DORA) for Resolving Spatial Overlaps in Individual-based Models of Microbes. *PLoS Computational Biology* (under review).
  7. Verhulst, A., Cappuyns, A., Van Derlinden, E., Bernaerts, K., & Van Impe, J. Analysis of the lag phase to exponential growth transition by incorporating inoculum characteristics. *Food Microbiology*, 28(4), 656–666 (2011).  
<https://doi.org/10.1016/j.fm.2010.07.014>
  8. Tack, I. L., Logist, F., Fernández, E. N., & Van Impe, J. F. An individual-based modeling approach to simulate the effects of cellular nutrient competition on *Escherichia coli* K-12 MG1655 colony behavior and interactions in aerobic structured food systems. *Food Microbiology*, 45, 179–188 (2015).  
<https://doi.org/10.1016/j.fm.2014.05.003>
  9. North, M. J., Collier, N. T., Ozik, J., Tatara, E. R., Macal, C. M., Bragen, M., et al. Complex adaptive systems modeling with Repast Symphony. *Complex Adaptive Systems Modeling*, 1(1), 3 (2013).  
<https://doi.org/10.1186/2194-3206-1-3>
  10. Picioreanu, C., Van Loosdrecht, M. C., & Heijnen, J. J. Mathematical modeling of biofilm structure with a hybrid differential-discrete cellular automaton approach. *Biotechnology and Bioengineering*, 58(1), 101–116 (1998).  
[https://doi.org/10.1002/\(sici\)1097-0290\(19980405\)58:1<101::aid-bit11>3.0.co;2-m](https://doi.org/10.1002/(sici)1097-0290(19980405)58:1<101::aid-bit11>3.0.co;2-m)

---

© 2025 by the authors. Licensed to PSEcommunity.org and PSE Press. This is an open access article under the creative commons CC-BY-SA licensing terms. Credit must be given to creator and adaptations must be shared under the same terms. See <https://creativecommons.org/licenses/by-sa/4.0/>

